ORIGINAL ARTICLE

NEUROPSYCHOPHARMACOLOGY REPORTS

WILEY

Effects of RORγt overexpression on the murine central nervous system

Tetsuya Sasaki[1,2] | Rei Nagata[1] | Satoru Takahashi[3] | Yosuke Takei[1,2]

[1]Faculty of Medicine, Department of Anatomy and Neuroscience, University of Tsukuba, Tsukuba, Ibaraki, Japan

[2]PhD Program of Neurosciences, Degree Program of Comprehensive Human Sciences, Graduate School of Comprehensive Human Sciences, University of Tsukuba, Tsukuba, Ibaraki, Japan

[3]Faculty of Medicine, Department of Anatomy and Embryology, University of Tsukuba, Tsukuba, Ibaraki, Japan

Correspondence
Tetsuya Sasaki and Yosuke Takei, Faculty of Medicine, Department of Anatomy and Neuroscience, University of Tsukuba, Tsukuba, Ibaraki, Japan.
Emails: tsasaki@md.tsukuba.ac.jp; ytakei@md.tsukuba.ac.jp

Abstract

Objective: T helper 17 (Th17) cells are a subset of CD4^{+} T cells that produce interleukin (IL)-17A. Recent studies showed that an increase in circulating IL-17A causes cognitive dysfunction, although it is unknown how increased systemic IL-17A affects brain function. Using transgenic mice overexpressing RORγt, a transcription factor essential for differentiation of Th17 cells (RORγt Tg mice), we examined changes in the brain caused by chronically increased IL-17A resulting from excessive activation of Th17 cells.

Results: RORγt Tg mice exhibited elevated *Rorc* and *IL-17A* mRNA expression in the colon, as well as a chronic increase in circulating IL-17A. We found that the immunoreactivity of Iba1 and density of microglia were lower in the dentate gyrus of RORγt Tg mice compared with wild-type mice. However, GFAP[+] astrocytes were unchanged in the hippocampi of RORγt Tg mice. Levels of synaptic proteins were not significantly different between RORγt Tg and wild-type mouse brains. In addition, novel object location test results indicated no difference in preference between these mice.

Conclusion: Our findings indicate that a continuous increase of IL-17A in response to RORγt overexpression resulted in decreased microglia activity in the dentate gyrus, but had only a subtle effect on murine hippocampal functions.

KEYWORDS

Astrocyte, Hippocampus, IL-17A, Microglia, RORγt

1 | INTRODUCTION

CD4^{+} helper T (Th) cells play an important role in immune responses by helping B cells and orchestrating CD8^{+} T cells and macrophages against pathogens. Functionally distinct subsets of Th cells produce different cytokines. One such subset is Th17 cells, whose signature cytokine is interleukin (IL)-17. IL-17 promotes inflammation by stimulating recruitment of neutrophils and monocytes[1], which are involved in autoimmune diseases such as rheumatoid arthritis, multiple sclerosis, and psoriasis[1-3]. Tumor growth factor β (TGF-β) and IL-6 are reportedly required for Th17 cell differentiation from naive T cells[4]. These mediators act in concert to activate the orphan nuclear receptor RORγt, a transcription factor indispensable for Th17 cell differentiation[5-7]. Th17 cells and IL-17A play a key role in neurological disorders such as multiple sclerosis, Alzheimer's disease, and schizophrenia through auto-inflammatory mechanisms[2]. In addition, IL-17 enhances microglial function[8] and activates astrocytes following spinal cord injury[9]. Recent research in mice indicates that maternal IL-17A promotes autism-related phenotypes in offspring by binding to IL-17 receptors on fetal cortical neurons[10,11], and an increase in circulating IL-17 leads to cognitive dysfunction by reducing nitric oxide production[12]. To investigate the effect of IL-17 on neuronal and glial cells in the brain, we made use of mutant mice overexpressing RORγt (RORγt Tg mice)[13,14]. As expected, these mice exhibited increased serum IL-17A levels compared with wild-type mice. Immunoreactivity of ionized calcium-binding adaptor molecule 1 (Iba1) and the density of microglia were unexpectedly decreased in the hippocampal dentate gyrus (DG) of RORγt Tg mice. However, despite the chronic increase in serum IL-17A in RORγt Tg mice, we found no changes in astrocytes, neurogenesis, hippocampal expression of synaptic molecules, or defects in spatial memory.

2 | MATERIALS AND METHODS

2.1 | Animals

RORγt Tg mice were generated on a C57BL/6 background in which transgene expression was driven by the CD2 promoter, a T-cell specific promotor[13,14]. The RORγt Tg mouse line was maintained by backcrossing with C57BL/6 mice. In this study, we used both male WT and RORγt Tg mice at 16W. All animals were housed under standard laboratory conditions (12/12 h light/dark cycle, free access to food and water) and maintained under pathogen-free conditions in the Laboratory Animal Resource Center at the University of Tsukuba. All animals received no treatment (including medication) prior to each experiment.

2.2 | Real-time PCR

Real-time PCR was performed as previously described[14]. Briefly, colon samples for real-time PCR experiments were obtained from 16W mice. Samples were collected with a Nucleocapsid RNA Kit (Macherey-Nagel, Düren, Germany), and RNA was extracted according to the manufacturer's instructions. Complementary DNA (cDNA) was generated from the obtained RNA with a High-Capacity RNA-to-cDNA kit (Thermo Fisher Scientific). For real-time PCR, cDNA samples were diluted and mixed with primer pairs for *Rorc* and *IL17A* (Table S1, Figure 1A), THUNDERBIRD SYBR qPCR mix, and H_2O. Twenty μL of each sample was placed in a PCR plate and run on an Eco Real-Time PCR System (Illumina, San Diego, CA). Quantification was performed by $2^{-\Delta\Delta Ct}$ analysis. Relative expression levels were calculated with the $2^{-\Delta\Delta Ct}$ method using *HPRT* as an internal control.

2.3 | Enzyme-linked immunosorbent assay (ELISA)

ELISA was performed as previously described[14]. Briefly, blood samples (>0.5 mL) were obtained from the hearts of male mice at 16W. Four mice per group (WT and RORγt Tg) were used for this analysis. The blood was collected in tubes (containing EDTA-2K and CJ-2DK; Terumo, Tokyo, Japan) and centrifuged at 3000 g at 4°C for 10 min. Serum concentrations of IL-6 and IL-17A were measured using an ELISA system according to the manufacturer's instructions (Figure 1B).

2.4 | Immunohistochemistry

For histological analysis, mice at 16W were deeply anesthetized with sodium pentobarbital (60 mg/kg body weight, intraperitoneal injection; Somnopentyl; BCM International, Hillsborough, NJ) and transcardially perfused with phosphate buffered saline (PBS), followed by 4% paraformaldehyde in 0.1 M phosphate buffer. Brain tissue sections (40 μm) were prepared with a sliding microtome (REM-710, Yamato-Kohki, Asaka, Japan) and stored at −20°C in cryoprotectant solution (30% glycerol, 30% ethylene glycol, and 40% 0.1 M phosphate buffer) until used in experiments.

Sections were rinsed three times with PBS, submerged in blocking solution (1% bovine serum albumin, 0.3% Triton-X 100, and 0.1% NaN$_3$ in PBS) for 60 min at room temperature, and then incubated with the following primary antibodies: Iba1 (1:2000, 019-19741, Fujifilm-Wako Pure Chemical, Tokyo, Japan), GFAP (1:1000, Rb-Af800, Frontier Institute), and DCX (1:2000, AB2253, Millipore). Sections were washed three times with PBS before incubating with secondary antibodies in an opaque container for 4 h at room temperature. Secondary antibodies used were goat anti-rabbit Alexa Fluor 488 (1:500, A11070, Thermo Fisher Scientific) and goat anti-guinea pig Alexa Fluor 488 (1:500, 1 938 425, Thermo Fisher Scientific). Slides were then washed four times with PBS containing 0.05% Tween-20 and mounted with PermaFluor (Thermo Fisher Scientific). Fluorescent images were acquired on an All-in-One Fluorescence Microscope BZX-710 with a 40 × objective lens using the Perfect Focus System (Figure 2A,D). Two regions of hippocampus, the DG and CA1, were examined in this study. Fluorescence
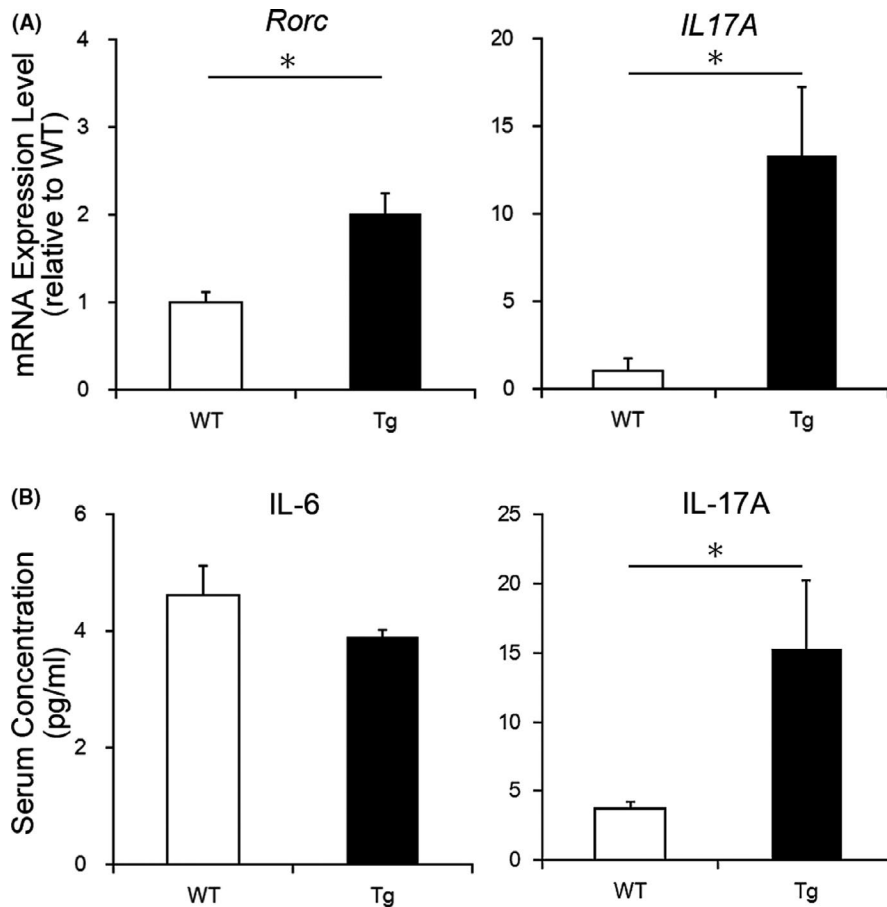
FIGURE 1 (A) mRNA expression levels of *Rorc* (left) and *IL17A* (right) in colon (n = 4 per group, two-way ANOVA, *P < 0.05). The *Rorc* gene encodes RORγt. *Rorc* and *IL17A* mRNA expression levels were significantly higher in the colon of RORγt Tg mice compared with WT mice. (B) Concentrations of IL-6 (left; n = 4 per group) and IL-17A (right) in serum (n = 3 in WT and n = 4 in Tg, *P < 0.05). Serum IL-17A concentrations were significantly higher in RORγt Tg compared with WT mice

intensities of Iba1$^+$ and GFAP$^+$ cells (Figure 2B,E), as well as the density of Iba1$^+$, GFAP$^+$, and DCX$^+$ cells (Figure 2C,F,H) were quantified with the microscope-integrated application. This analysis was carried out under the support of the Open Facility, Research Facility Center for Science and Technology, University of Tsukuba.

2.5 | Western blotting

Hippocampal tissue samples were collected from RORγt Tg and WT mice at 16W. Samples were homogenized and lysed in radioimmunoprecipitation assay buffer. Equal volumes were mixed with Laemmli sample buffer (Bio-Rad, Hercules, CA), boiled, and analyzed on 8%-10% sodium dodecyl sulfate polyacrylamide gels. Proteins were transferred to polyvinylidene difluoride membranes and blocked with 5% skim milk in Tris-buffered saline containing Tween-20 (TBST). Anti-NR2B (rabbit polyclonal, A-6474, 1:500; Thermo Fisher Scientific), anti-NR2A (rabbit polyclonal, 1:500, A-6476, Thermo Fisher Scientific), anti-PSD-95 (mouse monoclonal, 1:2000, ab13552; Abcam), and anti-PSD-93 (rabbit polyclonal, 1:1000, AB_2571834; Frontier Institute) diluted with 1% skim milk in TBST were used as primary antibodies and for overnight incubation. For normalization of proteins in each sample, α-tubulin (1:1000, T9026; Sigma-Aldrich) was used as a control (Figure 2J). Membranes were washed with TBST and incubated with goat anti-guinea pig secondary antibody conjugated to horseradish peroxidase (HRP) (1:10 000,

GR3175094-7, Abcam), anti-mouse secondary antibody conjugated to HRP, or anti-rabbit secondary antibody conjugated to HRP (1:10 000, 7076 and 7074, respectively; Cell Signaling Technology, Danvers, MA). Membranes were washed in TBST, and protein bands were visualized with Immobilon Western Chemiluminescent HRP Substrate (Millipore) using a LI-COR C-Digit Blot Scanner with Image Studio software (LI-COR, Lincoln, NE, USA).

2.6 | Behavioral analysis

Novel object location testing was performed as previously described with slight modifications[15]. Two-cylinder blocks were used as objects (Figure 3A). The placement apparatus consisted of an open field arena measuring 47 × 68 × 22 cm, with a black background. Two-cylinder blocks were used as objects, and each block was placed in the middle of the designated area to produce a symmetric appearance. The arena was set up under an overhead digital camera, and mice were tracked and recorded with automated tracking software. On Day 1 of the novel object location test, a single mouse was placed in the arena and its behavior was recorded for 10 min. Left and right blocks were placed symmetrically to each other (Figure 3A). The arena was cleaned with water and dried between each test subject to prevent any odor cues from previous subjects. On Day 2, the task was repeated with the right block placed at a different location (Figure 3A). This behavioral test primarily evaluates spatial learning,
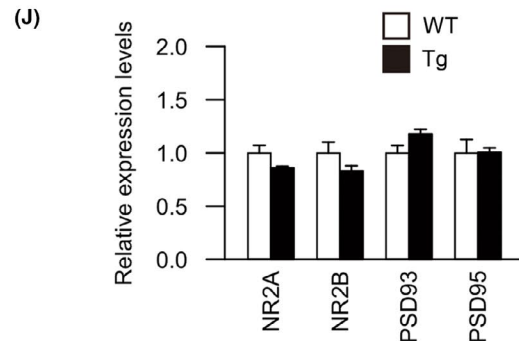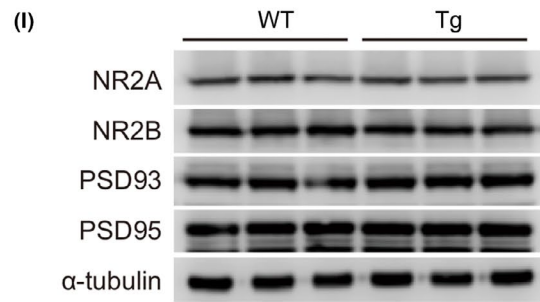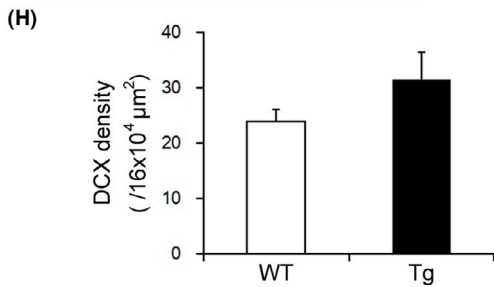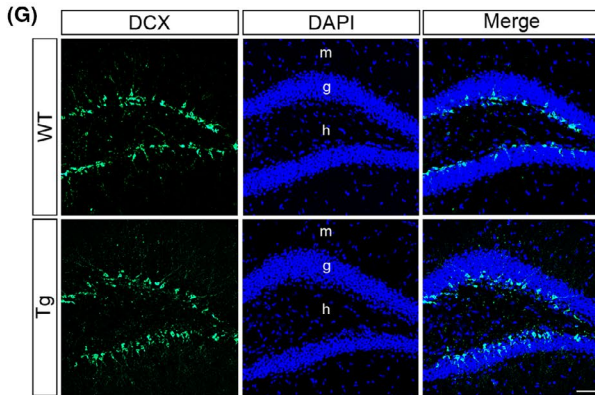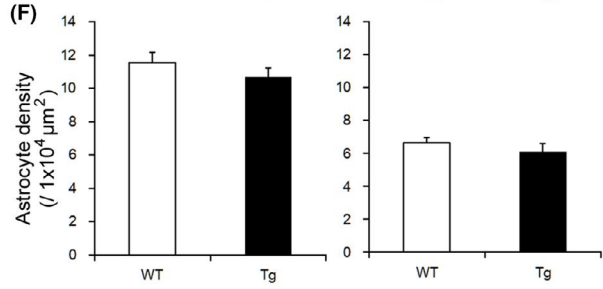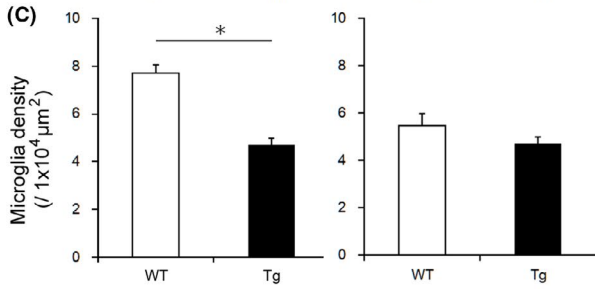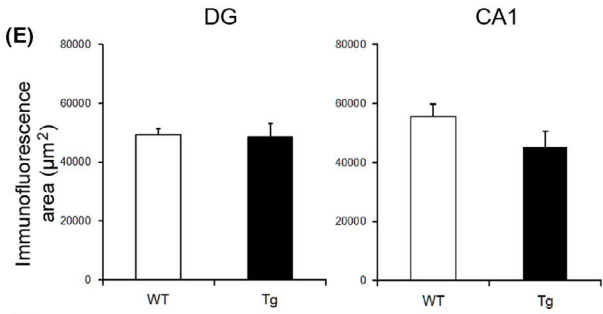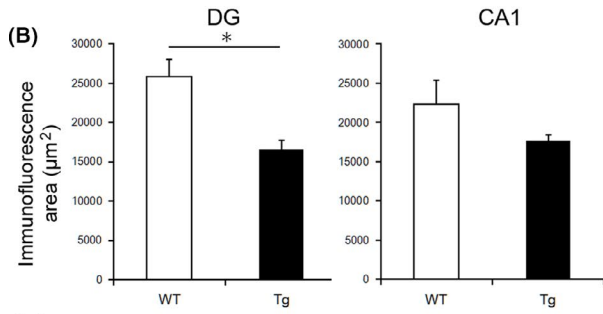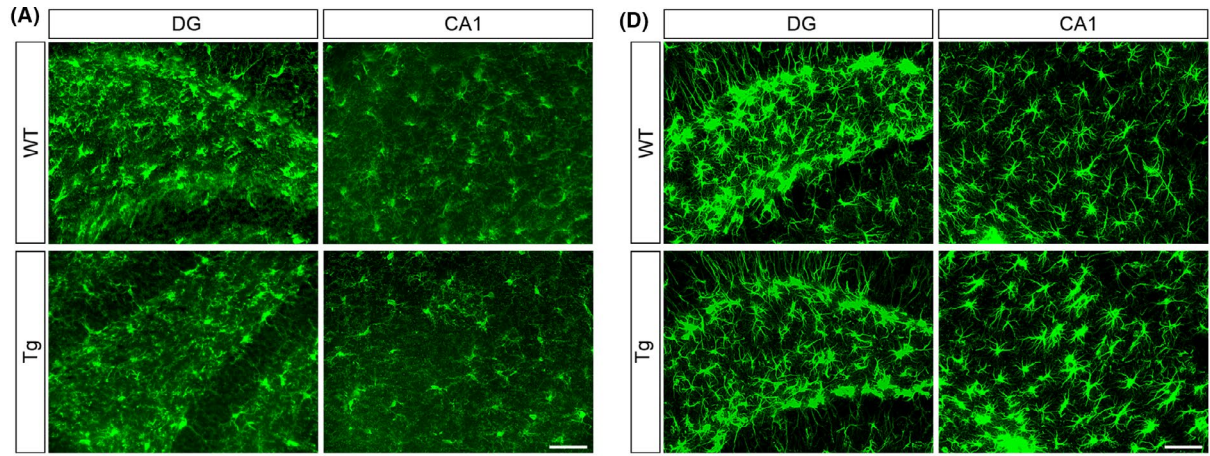
FIGURE 2 (A) Representative images of immunohistochemistry of Iba1 in the DG (left) and CA1 (right) regions of WT (upper panel) and RORγt Tg (lower panel) mice. (B) Semi-quantitative results of Iba1 immunofluorescence in DG (left) and CA1 (right) of WT and RORγt Tg mice (n = 3 per group, *$P < 0.05$). (C) Density of Iba1$^+$ microglia in the DG (left) and CA1 (right) of WT and RORγt Tg mice (n = 3 per group, *$P < 0.05$). Microglial activity and density were significantly lower in the DG of RORγt Tg compared with WT mice. (D) Representative images of immunohistochemistry for GFAP in DG (left) and CA1 (right) regions of WT (upper panel) and RORγt Tg (lower panel) mice. (E) Semi-quantitative results of GFAP immunofluorescence in the DG (left) and CA1 (right) of WT and RORγt Tg mice (n = 3 per group). (F) Density of GFAP$^+$ astrocytes in the DG (left) and CA1 (right) of WT and RORγt Tg mice (n = 3 per group). There were no significant differences in astrocyte activity or density between RORγt Tg and WT mice. (G) Representative images of immunohistochemistry of DCX (green) and DAPI (blue) in DG regions of WT (upper panel) and RORγt Tg (lower panel) mice. (H) Density of DCX$^+$ immature neurons in the DG of WT and RORγt Tg mice (n = 4 per group). (I) Western blot of synaptic molecules (NR2A, NR2B, PSD-93, and PSD-95) in the hippocampi of WT (left) and RORγt Tg (right) mice. For normalization of proteins in each sample, α-tubulin was used as a control (the lowest band). Each lane corresponds to a sample derived from one mouse (n = 3 per group). (J) Comparison of relative expression levels of NR2A, NR2B, PSD-93, and PSD-95 between WT and RORγt Tg mice (n = 3 per group). Scale bars = 50 μm
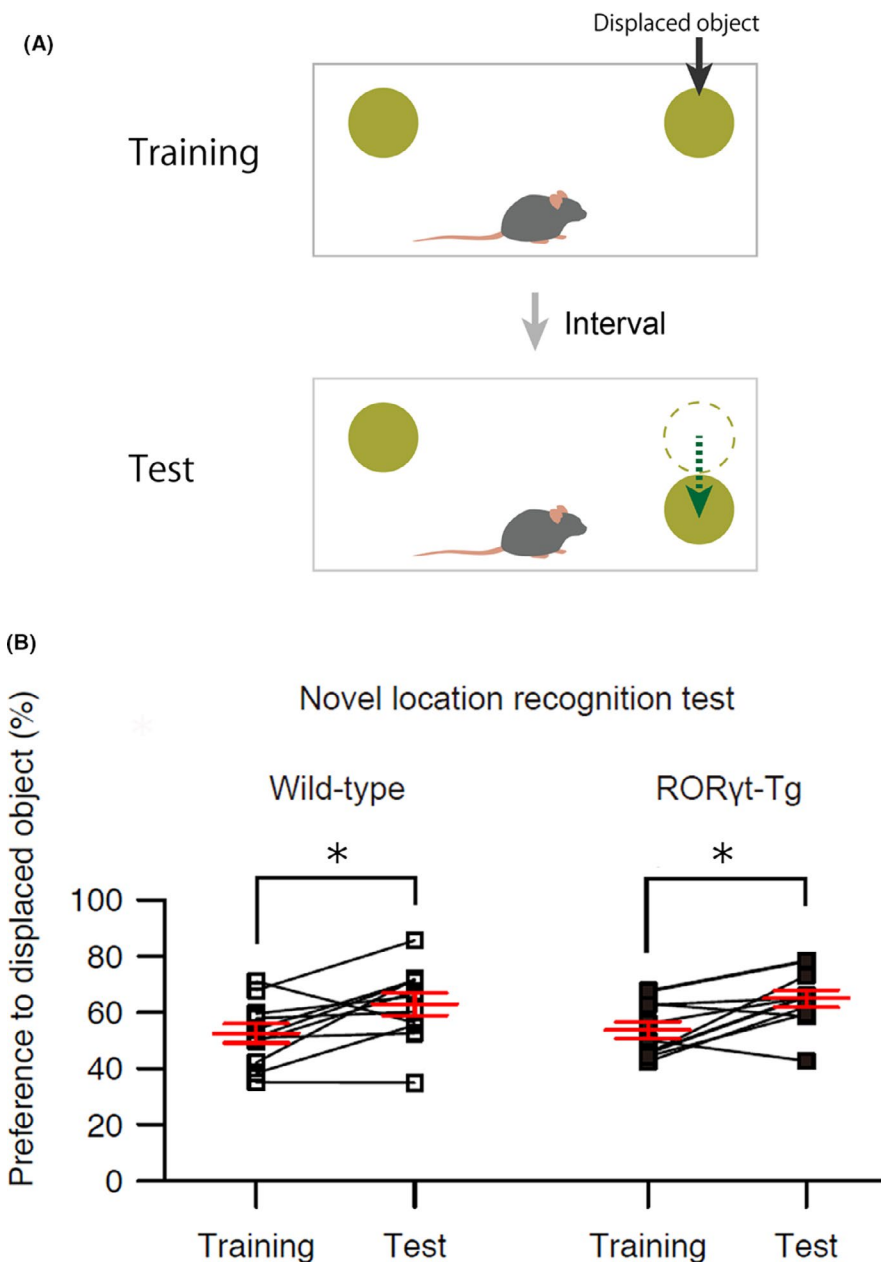
FIGURE 3 (A) Schematic of novel location recognition test. On Day 1, a single mouse was placed in the arena. Left and right blocks (green) were placed collinear to each other. On Day 2, the task was repeated with the right block placed at a different location (dotted arrow). (B) Percentages of preference for the displaced object. Both WT and RORγt Tg mice showed a preference for the object moved to a novel location. The level of preference was not different between WT and RORγt Tg mice. Two-way ANOVA, *$P < 0.05$

which relies on hippocampal activity. Only male mice at 16W were used for this test. Quantitative analysis of the retrieved data was performed using EthoVision XT (Noldus, Wageningen, Netherlands).

2.7 | Statistical analysis

Differences between the two groups were analyzed with Student's t test. Probability values < 0.05 were considered significant. Two-way analysis of variance (ANOVA) and Shaffer's modified sequentially rejective Bonferroni post hoc test was used for the mRNA expression level (Figure 1A) and novel location recognition test (Figure 3). Probability values < 0.1 were considered marginally significant, and probability values < 0.05 were considered significant. All data are expressed as mean ± standard error of the mean.

3 | RESULTS

3.1 | Elevated levels of *Rorc* and *IL17A* mRNA and serum IL-17A in RORγt Tg mice

Th17 cells are constitutively present in lamina propria of the gut[16,17] and differentiate from naive T cells upon stimulation with IL-6 and TGF-β[18]. mRNA levels of *Rorc* (the gene encoding RORγt) and *IL17A* were determined by qPCR and compared between RORγt Tg and wild-type (WT) mice (Figure 1A). In the colon, levels of both *Rorc* and *IL17A* mRNA were significantly higher in RORγt Tg mice compared with WT mice (Figure 1A, n = 4, $P < 0.05$). Consistently, IL-17A concentrations were significantly higher in RORγt Tg mice compared with WT mice (Figure 1B, 2.72 ± 1.11 vs 9.54 ± 1.77 pg/mL, respectively; $P < 0.05$); however, levels of IL-6 were unaltered (Figure 1B, 3.91 ± 0.11 vs 4.63 ± 0.49 pg/mL, respectively). These results indicate significantly elevated serum levels of IL-17A in RORγt Tg mice, which occurred concomitantly with upregulation of *Rorc* and *IL-17A* mRNA in the bowel.

3.2 | Microglia and astrocytes in the hippocampus of RORγt Tg mice

IL-17A binds to a receptor complex of IL-17 receptor subunit A (IL-17RA) and IL-17RC[19]. In the mouse brain, IL-17RA is expressed in microglia[20,21]. To investigate potential cellular alterations induced by overexpression of RORγt in the mouse brain, we visualized microglia and astrocytes using immunohistochemistry in RORγt Tg mice (Figure 2A,D).

Fluorescence intensity of Iba1, a marker of microglia/macrophage, was significantly decreased in the DG of RORγt Tg mice compared with WT mice (Figure 2B, 16 571.93 ± 1150.53 vs 25 387.14 ± 1706.29, respectively; $P < 0.05$). However, no significant difference in fluorescence intensities was observed in the cornu ammonis 1 (CA1) region of the hippocampus between RORγt Tg and

WT mice (Figure 2B, 15 245.00 ± 1302.7 vs 17 636.00 ± 817.87, respectively; $P = 0.18$). Accordingly, the density of Iba1+ cells was significantly decreased in the DG of RORγt Tg mice compared with WT mice (Figure 2C, 4.71 ± 0.27 vs 7.71 ± 0.36/10^4 μm², respectively; $P < 0.05$), but not in the CA1 (6.11 ± 0.51 vs 5.47 ± 0.52/10^4 μm², respectively; $P = 0.17$), without any marked morphological changes. Thus, the activity and density of Iba1+ microglia was specifically reduced in the DG of RORγt Tg mouse brains.

Immunofluorescence intensity of GFAP, a marker of astrocyte activation, was unaltered in the hippocampal DG and CA1 of RORγt Tg mice compared with WT mice (Figure 2E, DG: 49 249.33 ± 202.19 vs 48 719.25 ± 4324.98, respectively; $P = 0.93$; CA1: 25 387.14 ± 1706.29 vs 16 571.93 ± 1150.53, respectively; $P = 0.17$). There was also no difference in the density of GFAP+ astrocytes between WT and RORγt Tg mice (Figure 2F, DG: 11.56 ± 0.63 vs 10.67 ± 0.57/10^4 μm², respectively; $P = 0.93$; CA1: 6.11 ± 0.51 vs 6.67 ± 0.29/10^4 μm², respectively; $P = 0.31$). No substantial changes were observed in the activity or density of GFAP+ astrocytes in these hippocampal regions of RORγt Tg mice despite constitutively high levels of serum IL-17A.

Activation of microglia causes a decrease in the number and activity of stem cells, thereby reducing neurogenesis in the DG[22,23]. To evaluate the potential effects of altered glial-cell activity on neurogenesis in the brains of RORγt Tg mice, we performed immunohistochemistry with an antibody against DCX, a marker of immature neurons (Figure 2G). The density of DCX+ neurons was almost the same in WT and RORγt Tg mice (Figure 2H, 23.88 ± 2.34 vs 31.63 ± 4.79/10^4 μm², respectively; $P = 0.157$), indicating that reduced microglial activity does not affect neurogenesis in the DG of adult RORγt Tg mice.

3.3 | Hippocampal levels of synaptic molecules were maintained in RORγt Tg mice

To examine potential changes in synaptic molecules in response to a constitutive increase of IL-17A in RORγt Tg mice, Western blot analysis was performed using hippocampal tissues (Figure 2I). Protein levels of N-methyl-D-aspartate (NMDA) receptor subunits NR2A and NR2B, which are important for synaptic plasticity [24], and postsynaptic density proteins PSD93 and PSD95 were compared between RORγt Tg and WT mice. There was no significant difference in protein expression of these four synaptic molecules between RORγt Tg and WT mice (NR2A: $P = 0.130$; NR2B: $P = 0.211$; PSD93: $P = 0.101$; and PSD95: $P = 0.964$).

3.4 | Object location recognition testing revealed no difference in preference between WT and RORγt Tg mice

To examine whether increased IL-17A and microglial alterations in RORγt Tg mice influenced hippocampus-dependent brain function,

an object location recognition test was performed [15]. There was no difference among the genetic types in the preference to displaced object [two-way ANOVA; effect of genetic type: $F_{(1, 40)} = 0.21$, $P = 0.65$]. There was difference in the interaction between genetic type and test [two-way ANOVA; genetic type × test interaction: $F_{(3, 40)} = 3.53$, $P < 0.05$]. RORγt Tg mice exhibited preference to the displaced object to the same extent as WT mice (Figure 3, two-way ANOVA; effect of test: $F_{(1, 40)} = 10.36$, $P < 0.05$). These results suggest that RORγt Tg mice have normal hippocampus-dependent spatial memory function.

4 | DISCUSSION

In this study, to evaluate the effects of long-term upregulation of IL-17A on the CNS in vivo, we used transgenic mice overexpressing RORγt[13,14]. Serum levels of IL-17A in RORγt Tg mice were found to be elevated to three or more times the expected level, indicating that differentiation of Th17 cells is accelerated in response to overexpression of *Rorc* (*RORγt*), and IL-17A was excessively produced. We concentrated our analysis on the hippocampus of RORγt Tg mice.

Astrocytes are associated with the blood-brain barrier, causing them to confront infiltrating molecules into the CNS; thus, they may detect and be more sensitive to changes in IL-17 levels. Activation of astrocytes affects microglial function during neuroinflammation[25]. Contrary to our expectation, we did not observe any differences in the fluorescence intensity or density of GFAP+ astrocytes in RORγt Tg mice. However, the activity of Iba1+ microglia, which express IL-17RA[20,21], was significantly downregulated in the DG of RORγt Tg mice. In DG, the mean intensity of Iba1 per cell was almost the same between RORγt Tg (3.52) and WT (3.29), which indicates that the decrease in the number of Iba1+ cells intensely occurs in this area. In this regard, our previous study demonstrated that continuous elevation of IL-17A weakens poly(I:C)-mediated inflammatory responsiveness during pregnancy[14]. The interactions of Th17 and Tregs are bidirectional, and activated Th17 promotes the expansion and phenotype stability of Tregs[26]. Th17 produces high levels of TNF, which activates Tregs through the TNF-TNFR2 pathway[27]. The activity of Treg cells can lead to immunosuppression and a decrease in the number of Th1[28], which activates macrophages and microglia[29,30]. Thus, it is possible that persistently high levels of IL-17A activate inhibitory immune system responses and suppress microglial activity. Multiple regulatory pathways inhibit IL-17, including Th1, Th2, and regulatory T (Treg) cells, and interleukins such as IL-4 and interferon γ[14]. Among these regulatory systems, the balance between Th17 and Treg cells is important for the regulation of Th17-related immune responses. We considered that a continuous excess of Th17 cells caused by RORγt overexpression might potentiate these inhibitory systems and cytokines other than IL-17, such as IL-10, could be responsible for the observed hypoactivity of microglia.

We found no alterations in neurogenesis or levels of synaptic proteins in RORγt Tg mice. As inflammation may cause cognitive dysfunction, we expected to observe changes in expression of synaptic molecules between RORγt Tg and WT mice. These results suggest that the level of inflammation induced by elevation of IL-17A was not enough to cause robust changes in synaptic structure or function in the hippocampus of RORγt Tg mice.

Th17 cell–mediated inflammatory responses contribute to disruption of blood-brain barrier integrity and can cause cognitive impairment[31,32]. A previous work reported a breakdown of BBB because of the migration of Th17 cells from nose into brain in a mouse model of multiple group A Streptococcus[33]. As for IL-17, it was reported that tight junctions of endothelial cells were disrupted by IL-7-mediated inflammation in experimental autoimmune encephalomyelitis, an animal model of multiple sclerosis[34]. In the current work, we have not examined the status of BBB, which we would like to investigate as a future project.

In conclusion, our data indicate that chronically increased levels of IL-17A elicited by overexpression of RORγt resulted in reduced microglial activity in the DG, with subtle effects on murine hippocampal functions. Future work is necessary to elucidate the details of regulatory immune systems responsible for the brain phenotypes of microglia in RORγt Tg mice.

5 | LIMITATIONS

In the present study, we used early aged mice of 16W. Therefore, the factor of aging may influence the state of chronic inflammation. By using additional age groups, it may be able to more clearly delineate the effect of chronic inflammation due to excess IL-17A on the nervous system. The expression levels of synaptic molecules throughout the hippocampus may not reflect any difference in the expression levels of these molecules in the dentate gyrus. In addition, a more complicated test set, such as the Morris water maze, could be used to further examine behavior. Because this test takes several days to perform, differences between groups can be visualized in more detail.

CONFLICT OF INTEREST
The authors declare that the research was conducted in the absence of any commercial or financial relationship that could be construed as a potential conflict of interest.

AUTHOR CONTRIBUTIONS

ETHICS APPROVAL

DATA AVAILABILITY STATEMENT

ORCID

Tetsuya Sasaki https://orcid.org/0000-0002-7723-4417
Satoru Takahashi https://orcid.org/0000-0002-8540-7760
Yosuke Takei https://orcid.org/0000-0002-5026-8027

REFERENCES

1. Ishigame H, Kakuta S, Nagai T, Kadoki M, Nambu A, Komiyama Y, et al. Differential roles of interleukin-17A and -17F in host defense against mucoepithelial bacterial infection and allergic responses. Immunity. 2009;30:108–19.
2. Langrish CL, Chen YI, Blumenschein WM, Mattson J, Basham B, Sedgwick JD, et al. IL-23 drives a pathogenic T cell population that induces autoimmune inflammation. J Exp Med. 2005;201:233–40.
3. Pène J, Chevalier S, Preisser L, Vénéreau E, Guilleux M-H, Ghannam S, et al. Chronically inflamed human tissues are infiltrated by highly differentiated Th17 lymphocytes. J Immunol. 2008;180:7423–30.
4. Bettelli E, Carrier Y, Gao W, Korn T, Strom TB, Oukka M, et al. Reciprocal developmental pathways for the generation of pathogenic effector TH17 and regulatory T cells. Nature. 2006;441:235–8.
5. Ivanov II, McKenzie BS, Zhou L, Tadokoro CE, Lepelley A, Lafaille JJ, et al. The orphan nuclear receptor RORgammat directs the differentiation program of proinflammatory IL-17+ T helper cells. Cell. 2006;126:1121–33.
6. Ivanov II, Atarashi K, Manel N, Brodie EL, Shima T, Karaoz U, et al. Induction of intestinal Th17 cells by segmented filamentous bacteria. Cell. 2009;139:485–98.
7. Kleinewietfeld M, Manzel A, Titze J, Kvakan H, Yosef N, Linker RA, et al. Sodium chloride drives autoimmune disease by the induction of pathogenic TH17 cells. Nature. 2013;496:518–22.
8. Kawanokuchi J, Shimizu K, Nitta A, Yamada K, Mizuno T, Takeuchi H, et al. Production and functions of IL-17 in microglia. J Neuroimmunol. 2008;194:54–61.
9. You T, Bi Y, li J, Zhang M, Chen X, Zhang K, et al. IL-17 induces reactive astrocytes and up-regulation of vascular endothelial growth factor (VEGF) through JAK/STAT signaling. Sci Rep. 2017;7:41779.
10. Choi GB, Yim YS, Wong H, Kim S, Kim H, Kim SV, et al. The maternal interleukin-17a pathway in mice promotes autism-like phenotypes in offspring. Science. 2016;351:933–9.
11. Reed MD, Yim YS, Wimmer RD, Kim H, Ryu C, Welch GM, et al. IL-17a promotes sociability in mouse models of neurodevelopmental disorders. Nature. 2020;577:249–53.
12. Faraco G, Brea D, Garcia-Bonilla L, Wang G, Racchumi G, Chang H, et al. Dietary salt promotes neurovascular and cognitive dysfunction through a gut-initiated TH17 response. Nat Neurosci. 2018;21:240–9.
13. Yoh K, Morito N, Ojima M, Shibuya K, Yamashita Y, Morishima Y, et al. Overexpression of RORgammat under control of the CD2 promoter induces polyclonal plasmacytosis and autoantibody production in transgenic mice. Eur J Immunol. 2012;42:1999–2009.
14. Tome S, Sasaki T, Takahashi S, Takei Y. Elevated maternal retinoic acid-related orphan receptor-gammat enhances the effect of polyinosinic-polycytidylic acid in inducing fetal loss. Exp Anim. 2019;68:491–7.
15. Vogel-Ciernia A, Wood MA. Examining object location and object recognition memory in mice. Curr Protoc Neurosci. 2014;69:1–17.
16. Weaver CT, Elson CO, Fouser LA, Kolls JK. The Th17 pathway and inflammatory diseases of the intestines, lungs, and skin. Ann Rev Pathol. 2013;8:477–512.
17. Atarashi K, Tanoue T, Ando M, Kamada N, Nagano Y, Narushima S, et al. Th17 cell induction by adhesion of microbes to intestinal epithelial cells. Cell. 2015;163:367–80.
18. Miossec P, Kolls JK. Targeting IL-17 and TH17 cells in chronic inflammation. Nat Rev Drug Discovery. 2012;11:763–76.
19. Gaffen SL. Structure and signalling in the IL-17 receptor family. Nat Rev Immunol. 2009;9:556–67.
20. Sarma J, Ciric B, Marek R, Sadhukhan S, Caruso ML, Shafagh J, et al. Functional interleukin-17 receptor A is expressed in central nervous system glia and upregulated in experimental autoimmune encephalomyelitis. J Neuroinflammation. 2009;6:14.
21. Li Q, Cheng Z, Zhou LU, Darmanis S, Neff NF, Okamoto J, et al. Developmental heterogeneity of microglia and brain myeloid cells revealed by deep single-cell RNA sequencing. Neuron. 2019;101:207–23.e10.
22. Yousef H, Czupalla CJ, Lee D, Chen MB, Burke AN, Zera KA, et al. Aged blood impairs hippocampal neural precursor activity and activates microglia via brain endothelial cell VCAM1. Nat Med. 2019;25:988–1000.
23. Dalmau I, Finsen B, Zimmer J, Gonzalez B, Castellano B. Development of microglia in the postnatal rat hippocampus. Hippocampus. 1998;8:458–74.
24. Fox CJ, Russell KI, Wang YT, Christie BR. Contribution of NR2A and NR2B NMDA subunits to bidirectional synaptic plasticity in the hippocampus in vivo. Hippocampus. 2006;16:907–15.
25. Argaw AT, Asp L, Zhang J, Navrazhina K, Pham T, Mariani JN, et al. Astrocyte-derived VEGF-A drives blood-brain barrier disruption in CNS inflammatory disease. J Clin Investig. 2012;122:2454–68.
26. Chen X, Oppenheim JJ. Th17 cells and Tregs: unlikely allies. J Leukoc Biol. 2014;95:723–31.
27. Okubo Y, Mera T, Wang L, Faustman DL. Homogeneous expansion of human T-regulatory cells via tumor necrosis factor receptor 2. Sci Rep. 2013;3:3153.
28. Nedoszytko B, Lange M, Sokołowska-Wojdyło M, Renke J, Trzonkowski P, Sobjanek M, et al. The role of regulatory T cells and genes involved in their differentiation in pathogenesis of selected inflammatory and neoplastic skin diseases. Part I: Treg properties and functions. Postepy Dermatol Alerg. 2017;34:285–94.
29. Prajeeth CK, Kronisch J, Khorooshi R, Knier B, Toft-Hansen H, Gudi V, et al. Effectors of Th1 and Th17 cells act on astrocytes and augment their neuroinflammatory properties. J Neuroinflammation. 2017;14:204.
30. Prajeeth CK, Löhr K, Floess S, Zimmermann J, Ulrich R, Gudi V, et al. Effector molecules released by Th1 but not Th17 cells drive an M1 response in microglia. Brain Behav Immun. 2014;37:248–59.

31. Engelhardt B, Ransohoff RM. Capture, crawl, cross: the T cell code to breach the blood-brain barriers. Trends Immunol. 2012;33:579–89.

32. Cipollini V, Anrather J, Orzi F, Iadecola C. Th17 and cognitive impairment: possible mechanisms of action. Front Neuroanat. 2019;13:95.

33. Platt MP, Bolding KA, Wayne CR, Chaudhry S, Cutforth T, Franks KM, et al. Th17 lymphocytes drive vascular and neuronal deficits in a mouse model of postinfectious autoimmune encephalitis. Proc Natl Acad Sci USA. 2020;117:6708–16.

34. Rostami A, Ciric B. Role of Th17 cells in the pathogenesis of CNS inflammatory demyelination. J Neurol Sci. 2013;333:76–87.

SUPPORTING INFORMATION

Additional supporting information may be found online in the Supporting Information section.